Effect of the tire – Pavement contact at the surface layer when the tire is tilted in bend

Y. Oubahdou, E.-R. Wallace, P. Reynaud, B. Picoux, J. Dopeux, C. Petit, D. Nelias

Version of Record: https://www.sciencedirect.com/science/article/pii/S0950061821025198
Manuscript_9de78f909b98b4818283ea7409ed9273

Effect of the tire - pavement contact at the surface layer when the tire is tilted in bend

Y. Oubahdou[1], E-R. Wallace[2], P. Reynaud[1], B. Picoux[1], J. Dopeux[1], C. Petit[1*], D. Nélias[2],

1. *Université de Limoges, GC2D, EA 3178, F-19300 Egletons, France*
2. *Univ Lyon, INSA-Lyon, CNRS UMR5259, LaMCoS, F-69621, France*

*christophe.petit@unilim.fr

ABSTRACT

Tire-pavement interaction is a rolling contact problem that depends on tire and pavement factors, such as vehicle speed and weight, material and type of tire, tire pressure inflation, camber and texture of the surface layer. In this paper, the problem of tire-pavement contact is studied using a realistic description in normal section and bend. The study focuses on the shape of the contact patch and the stress distribution at the tire-pavement interface and the surface shear stresses rather than internal stresses in the structure of the pavement. The numerical approach introduced requires precise tire geometry (estimated by a photogrammetry method) and an equivalent Young's modulus (function of the inflation pressure resulting from the press load tests). Vertical contact stress at the tire-pavement interface predicted by a Semi-Analytical model were compared to experimental measurements with a press system under different loads and angles of inclination. Finally, we discuss the effect of the tire inclination on the calculated shear stresses (origins of damage in turns). The model shows that the increase of the angle of inclination in a turn has a direct influence on the distribution of the tire-pavement contact stresses and the shear stresses. These results will provide indications for the evaluation of the performance of the surface layer with respect to rutting and downward cracking.

Keywords: Surface layer, Tire-pavement contact, Tire inclination, Degradations, Semi Analytical Model

Declarations of conflicts of interest: None

ABSTRACT

The tire-pavement interaction is a rolling contact problem that depends on both tire and pavement factors, such as vehicle speed and weight, tire material and type, tire pressure inflation, and surface layer camber and texture. This paper studies the tire-pavement contact problem using a realistic description in the normal section and in a bend. The study focuses on the shape of the contact patch, as well as the stress distribution at the tire-pavement interface and the surface shear stresses rather than internal stresses within the pavement structure. The numerical approach introduced herein requires precise tire geometry and an equivalent Young's modulus value. The vertical contact stress at the tire-pavement interface predicted by a semi-analytical model is compared to experimental measurements conducted with a press system under various loads and angles of inclination. Moreover, the effect of tire inclination on the calculated shear stresses is discussed. The model shows that the increase in the angle of inclination in a turn has a direct influence on the distribution of the tire-pavement contact stresses and shear stresses. Through the tensile strain limit criterion ε_6 derived from pavement design method, these results provide indications for evaluating the performance of the surface layer with respect to rutting and downward cracking.

Keywords: Surface layer, Tire-pavement contact, Tire inclination, Degradations, Semi-analytical model

Introduction

The road design method assumes that the tire-pavement contact area is circular and contact pressure is evenly distributed. However, several datasets published from measurements and modeling of tire contact pressure show that the components of vertical stresses at the tire-road interface are not uniformly distributed (see [1-4]). In addition, shear stresses in the transverse and longitudinal directions lead to degradations of the surface layer, mainly at specific points where shear stresses are greater than in the normal section. One of the challenges of our research project is to study surface layer damage in the bend, as exemplified by the case where the trajectory changes and shear stresses might alter the prediction of top-down cracking, primary rutting and perhaps fatigue damage ([5-7]). Several works have introduced finite element studies on the contact conditions in bends by comparison with experimental validations ([7-9]). It has been found that the maximum vertical contact stress is located under the intermediate rib of the tire, instead of the central rib. This stress increases as the camber angle increases. Generally speaking, each rib of the tire behaves differently from the others, especially when the wheel is inclined (in a bend), leading to an asymmetry of the contact pressures in the central plane. Gruber et al. [10] explained this distribution by the deflections caused in each rib of the tire in the tread. Yanjin et al. [11] also studied the influence of the angle of banking experienced by a car wheel in a turn on the tire deflection. Both theoretical and experimental results have shown that the greater the camber angle, the greater the tire deflection under the same load. Hence, the vertical camber stiffness of a radial tire decreases with increasing camber angle. Zhou et al. [12] discussed the effect of friction on the contact conditions among the various rolling cases, namely tire inclination in a turn combined with the sliding condition. Other authors have demonstrated that the contact stress at the tire edge is greater than the central rib contact stress during tire inclination. Camber also changes the contact length of the tire edge while increasing stress values. Using a finite element calculation, Wang et al. ([11], [13]) and Vayalat [14] found the same result and concluded that the normal stress in the contact zone increases as the camber angle increases and is concentrated at the tire edge. It has also been shown that the non-uniformity of contact pressure combined with a differential slip along the width of the tire in a camber state can cause longitudinal resistance and camber alignment torque. Kageyama et al. [15] carried out calculations to evaluate the effect of tire inclination on several parameters, namely contact area, contact length and width, stiffness and lateral displacement, as well as the thrust and torque due to the inclination. These calculations were subsequently validated by several tests. Results indicated that tire inclination has both a qualitative and quantitative effect on the various examined parameters, in particular on contact pressure, which increases in intensity and changes shape as the camber angle increases.

This paper introduces an estimation of the contact pressure during a turn by means of simulation using a semi-analytical calculation (SAM). The position of the tire in inclined turns is subjected to a static vertical force. Next, this model is validated using an experimental method by measuring contact pressures under the same conditions using a pressure sensor (Tekscan). In parallel, the effect of tire inclination on the surface shear stresses is studied, primarily the transverse stresses and the longitudinal and transverse strains on the surface. The strain is validated by measurements with an innovative camera technique placed to the right of the inclined tire. Lastly, the maximum tensile strain at the surface is compared to the limit criterion ε_6 drawn from the pavement design method. These results provide indications for evaluating the surface layer performance.

1. Semi-analytical modeling of the tire-pavement contact

1.1. Objectives

Bends are more sensitive to surface shear failure and permanent strains than other common tire sections ([16], [17]), due to the magnitude of significant traffic-induced aggression (tangential force, axle load asymmetry). Since traffic loads are applied to the pavement by tires, we have chosen herein to analyze this pressure contact by means of a tribological approach based on a semi-analytical code. The model derived allows for the integration of the tire's actual geometry by both digitizing the tire profile using the photogrammetry method and hypothesizing it as an elastic linear homogeneous body modeled by an equivalent Young's modulus. Semi-analytical modeling simulates the road's surface stresses in a normal section and in a bend. In order to validate these numerical results, a 295 / 80R 22.5 tire with an inflation pressure of 820 kPa was used. In the normal section, the tire was loaded at 32.5 kN; the contact points were measured by a pressure sensor system (Tekscan). During gyrations, lateral load transfer tends to amplify the load on the outer wheel. To take this phenomenon into account, seven camber angle variants (0, 1, 2, 3, 4, 5 and 6 degrees) with the same 45-kN load were chosen. The pressures obtained were then validated with this same Tekscan system.

1.2. Modeling aspects

The study of pavement tire contact requires information on the size and shape of the contact area since the stresses are generated by their interaction. To solve this problem, the complexity of materials, geometry and tribology must all be considered. For this purpose, several experimental studies have been referenced to analyze the problem despite being limited by the cost and complexity of the test equipment. Numerical models based on the finite element method (FEM) have also been developed. Several works in the tire industry have led to high-precision simulations using 3D finite elements. Most of these calculations require an enormous amount of time (and are not really applicable in the road industry). In addition, these studies are generally limited to quasi-static or stationary stresses ([18]). A semi-analytical method, based on the summation of analytical solutions using digital techniques such as the Fourier Fast Transform (FFT) and the Conjugate Gradient Method (CGM), is indeed preferred by researchers. Such techniques were first proposed respectively by Liu ([19]) and Polonsky ([20]). Nélias et al. ([21-24]) developed a semi-analytical code from these techniques for any type of contact geometry, encompassing various material behaviors and loads. Experimental observations focus on the normal contact and derived pressure distribution. Figure 1 shows the tire/road contact under a normal force P. The surface has been discretized with rectangular elements of size dx × dy.

By assuming the two materials as linear, isotropic and homogeneous elastic, the normal contact problem can be formulated with the following points:

- Load balancing: the load P applied to the upper body (the tire in the present case) must be equal to the sum of the contact pressures distributed over the contact zone Γ_c.

$$\iint_{\Gamma_c} p(x,y)dxdy = P \quad (1)$$

- Separation of the bodies: the final separation of the bodies after loading ($g(x,y)$) is equal to the sum of the initial separation of the bodies ($h_i(x,y)$), the rigid body

displacement (δ) and the elastic displacement at the surfaces of the bodies in contact ($u_z(x,y)$).

$$g(x,y) = h_i(x,y) - \delta + u_z(x,y) \tag{2}$$

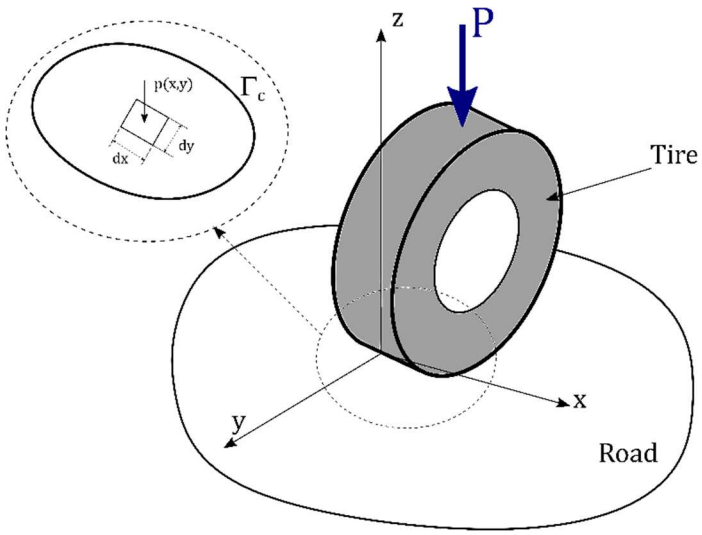

Fig. 1: Contact between tire and road under a normal force P, with a close-up of the contact zone Γ_c, which shows a surface element of size dx×dy

Let's note that elastic displacements at the surface are identified by using the Boussinesq [25] and Cerutti [26] potentials. Since the target surface has been discretized, Love's approach [27], which finds the potentials on a rectangular patch, can be used. Furthermore, convolutions with Fourier Transform properties are performed to seek the solution over the entire contact area.

Ultimately, the contact conditions read as follows:

$$p(x,y) > 0 \; ; \; g(x,y) = 0 \text{ in the contact zone} \tag{3}$$

$$p(x,y) = 0 \; ; \; g(x,y) > 0 \text{ outside of the contact zone} \tag{4}$$

At this point, the contact problem turns into a variational problem, whose solution is the pressure distribution that minimizes complementary energy (see Duvaut and Lions [28] for the variational formulation). Next, the CGM algorithm is applied to solve the contact (see Gallego [24] for the corresponding algorithm). Once the contact has been solved, the pressure distribution at the surface can be applied to find stresses over the entire road by means of convolution with the corresponding potentials. In addition, the geometries of the bodies in contact must be known in order to better approximate the distribution of contact pressures. Thus, in the case of tire-pavement contact, the tire geometry is reproduced according to a photogrammetric technique ([26]). The tire inclination is achieved by rotating the tire around its center line. The mechanical properties of the tire are determined by assimilating the tire to a solid cylinder and using a force-displacement model based on a linear contact, whose parameters are obtained by calibrating the results of forced experimental deviations. The tire is assumed to be incompressible. As explained above, this modeling approach relies on a two-layer tire, with considerations for the composite structure and anisotropy due to the significant

difference in stiffness between the rubber and the tire reinforcement. The tire structure considered herein consists of an initial 18-mm layer with a modulus of 12 MPa [7], while the thickness of the second layer is 200 mm with an estimated modulus of 3.694 MPa (see Fig. 2).

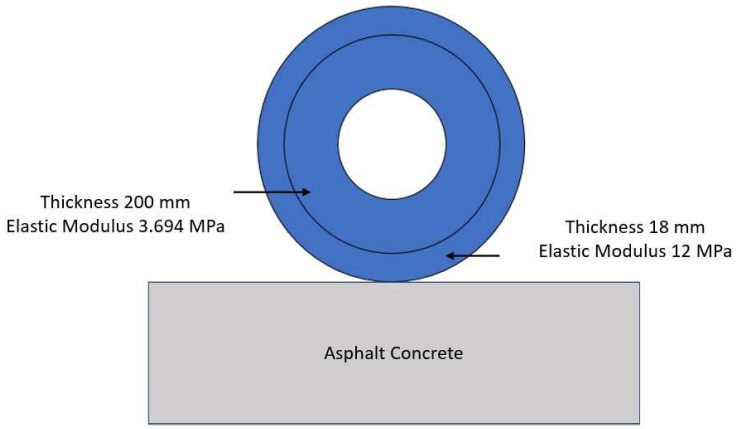

Fig. 2: Cross-section of the tire structure, indicating the parameters used in SAM

2. Experimental validation

2.1. Experimental set-up

To assess the accuracy of the model developed, the vertical contact stress predicted at the tire-pavement interface was compared to experimental measurements conducted using a pressure sensor system (Tekscan). The operating principle behind Tekscan (Fig. 3) is based on a resistive polymer whose electrical resistance changes as a function of the applied stress.

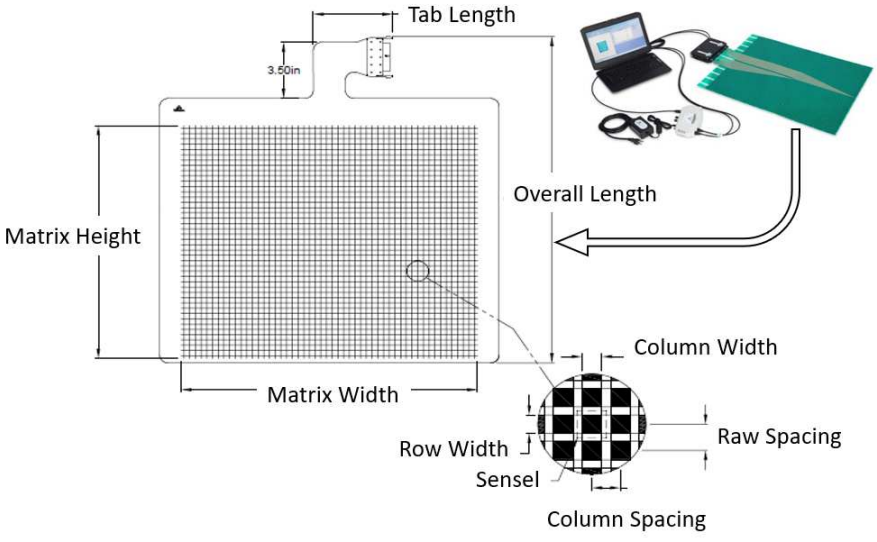

Fig. 3: Matrix of sensitive elements formed by Tekscan piezoresistive sensors (source: https://www.tekscan.com/)

This technique makes it possible to obtain measurements during both static and dynamic tests. The electronic sheet is incompressible and operates at temperatures of between -40° and 200°C, with a moisture percentage of 5% to 10%. Two polyester sheets were needed to build the sensor. On the first sheet, piezoresistive materials (sensors) were placed an equal distance

apart. On the second sheet, the same sensors were placed in the same layout, but perpendicular to the first sheet. These rows and columns of sensors intersected to form a matrix of tightly-spaced sensitive elements when the two sheets were joined. The typical accuracy of these sensors is ±5%, and the surface area of a sensor equals 25.806 mm^2 (or a 3-mm width separated by 2.08 mm). Thus, in the SAM simulation, a 3-mm mesh pitch in the longitudinal (x) and lateral (y) directions must be chosen. The Tekscan pressure sensor has been calibrated with a load of 45 kN under a Zwick press system. During calibration, the software calculates an average applied pressure based on both the loaded sensor area and applied force value.

2.2. Experimental protocol

In a roundabout, truck speed is generally low (5 to 30 km per hour), hence the load application takes longer than in a busy road section. However, because of its geometry and the effect of the centrifugal force resulting from the turn, the load distribution is unbalanced between wheels of the same axle. This imbalance is due to the drag of the wheel overload outside the turn (by 10% to 20% according to French measurements). Theoretically, it is assumed that during a turn, the tires of a vehicle are inclined at a camber angle with the road surface. This angle causes a difference in shear stress and vertical distribution of stresses in the road structure compared to straight sections or when the tires do not tilt without an inclination angle. To study and verify this hypothesis, several angles of tire inclination were chosen: 0, 2, 4, 5 and 6 degrees. These tests were carried out in a static state. The experimental protocol adopted to describe the contact pressures in bends and normal sections is based on measuring the contact pressure between a heavy vehicle tire (reference 295 / 80R 22.5) with an inflation pressure of 820 kPa. The material in contact with the tire was produced on a coated plate with a modulus of 5,400 MPa (20 cm thick). To simulate the tire position on a turn under the press, the principle of the inclinometer (see Fig. 4) has been applied.

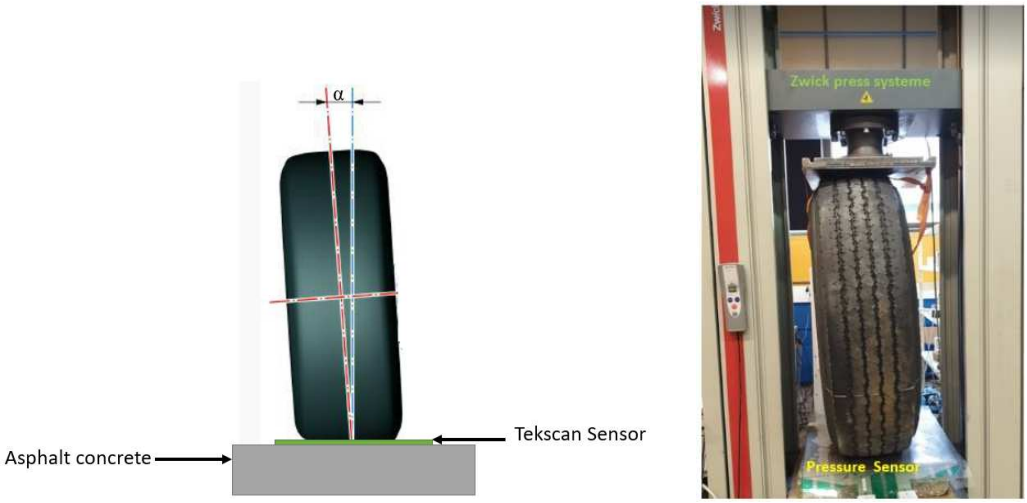

Fig. 4: Experimental protocol of an inclined tire under the press

The angles have been arbitrarily selected in order to conservatively cover the theoretical worst-case range for tire tilt angles at roundabouts, with measurements performed during each loading test. In the normal section, the tire was loaded at 32.5 kN and the contact pressures were measured by the Tekscan sensor system. In the roundabout, the lateral load tends to amplify loading on the outer wheel; hence, we proposed for the tire to be loaded with a static

charge of 45 kN. The pressures obtained have been validated with the same Tekscan measuring system.

3. Analysis and discussion

3.1. Vertical contact stress at zero tire inclination

Figure 5 shows the distribution of the contact pressure field for a 32.5-kN normal static load at 0° inclination. A relatively good correspondence is observed between the numerical and experimental results, especially in terms of average maximum pressures. The average maximum measured value is 1,400 kPa and the maximum value calculated equals 1,536 kPa. Moreover, it can be observed that the contact pressure distributions are nearly identical. The contact area calculated with SAM is 42,870 mm^2 and that measured with Tekscan is 43,974 mm^2.

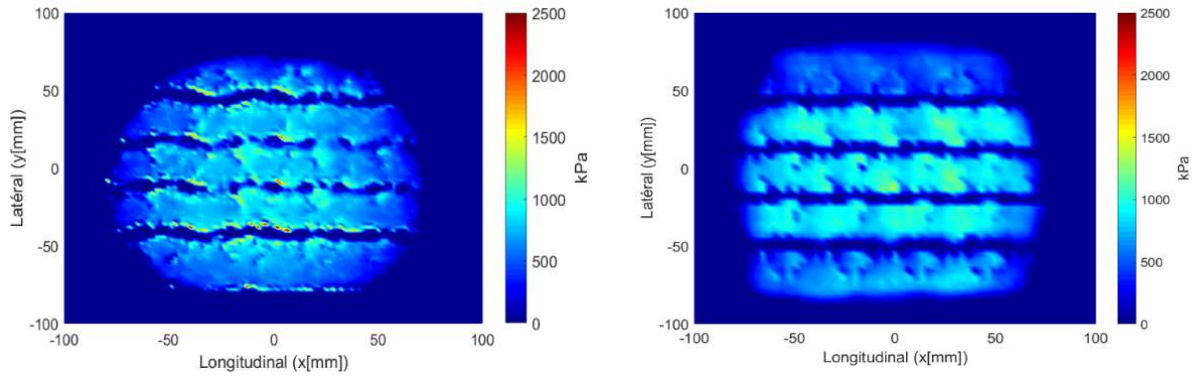

Fig. 5: Results for 0° inclinations: (right) Tekscan measurement, (left) SAM simulation

3.2. Vertical contact stress for the tire inclination

Figure 6 shows the results for several degrees of inclination (from 2° to 6°); the applied load of the tires in bends is 45 kN with a tire inflation pressure of 820 kPa. For 2° inclinations, the average maximum stress is 1,591 kPa from measurements and 1,650 kPa output from the calculation code. The contact pressure profiles for the two existing inclinations appear to be the same. The contact area calculated with SAM is 52,370 mm² and that measured with Tekscan 53,471 mm^2. At 4°, a decrease is noticed in the contact area compared to 2°: the contact area calculated with SAM is 51,581 mm^2 while that measured with Tekscan is 52,748 mm^2. The maximum pressure is always located at the edge of the tire, and the average maximum stress is 1,788 kPa from measurements and 1,850 kPa from the calculation code. At 5°, the maximum pressure measured climbs to 2,100 kPa vs. 1,895 kPa calculated using the SAM code. At 6°, a slight increase in contact area compared to 5° can be observed, with the maximum contact pressures once again localized at the edges of the tire. This result enhances the theoretical hypothesis that the turning point can cause greater stress on pavement. It is also observed that the distributions of contact pressures are nearly identical (calculations and measurements). On a normal section, the shape of the contact zone between the pavement tire is rectangular, and the maximum value of the contact stress appears at or close to the center of the contact zone. The contact zone seems to be reduced and the contact surface becomes trapezoidal during turns.

246

247

	SAM simulation	*Tekscan measurement*
2° inclination	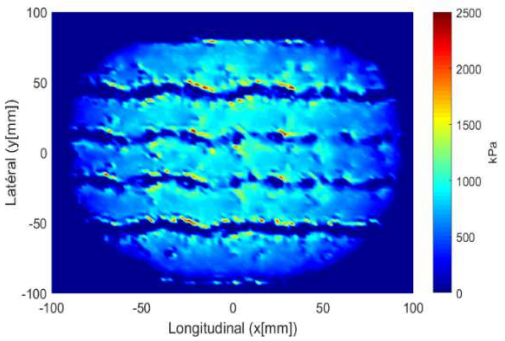	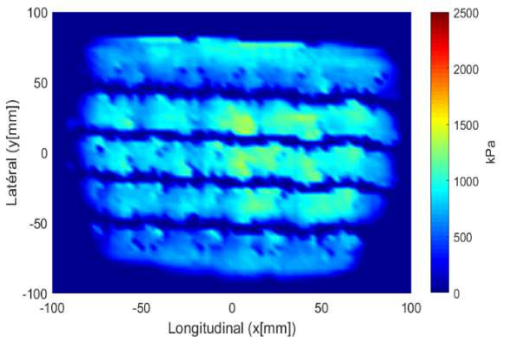
4° inclination	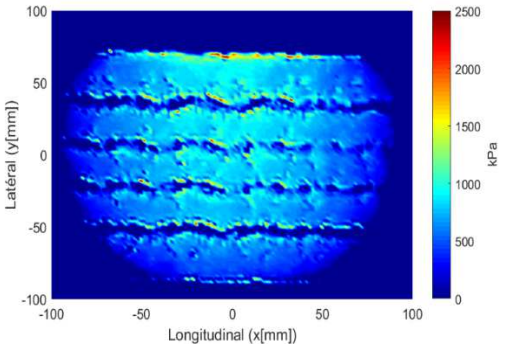	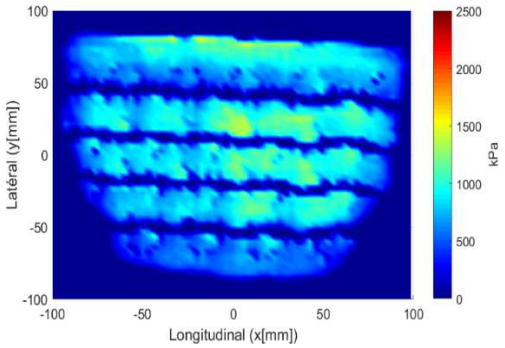
5° inclination	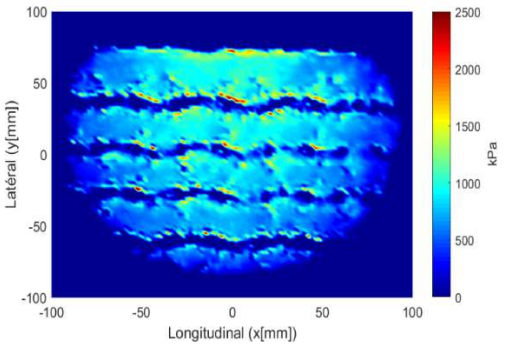	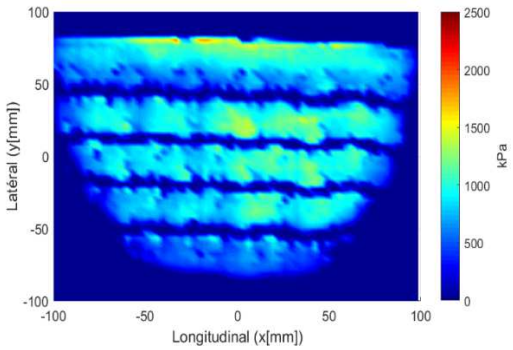

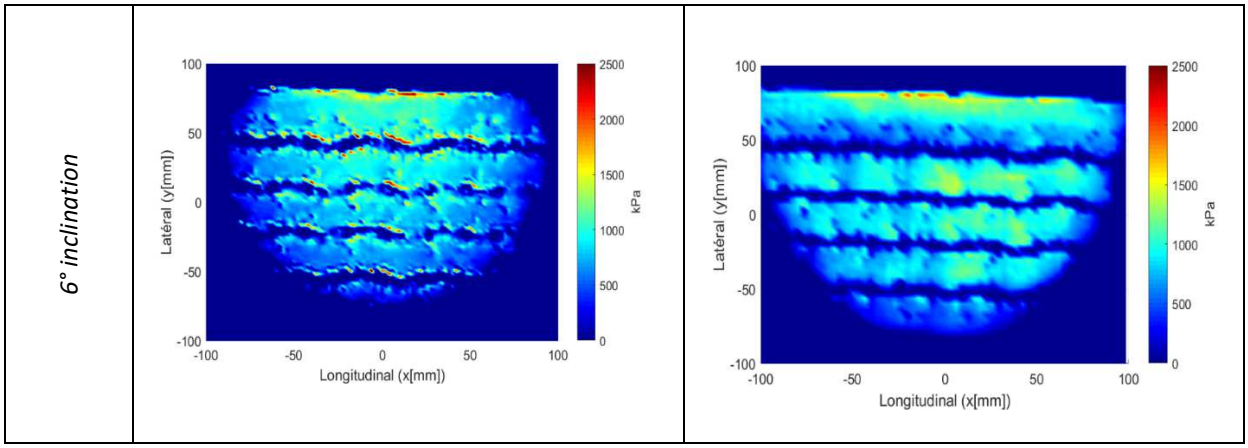

Fig. 6: Contact pressure at several degrees of inclination

For the various angles of inclination, these results show that the tire inclination in bends causes a concentration of contact stresses to the right of the road contact zone. This location lies on the inner side of the turn, which means that the right shoulder of the tire is compressed more than the left shoulder when cornering. Results from the SAM model allow for comparison with the measurement values listed in Table 1. The contact area and average maximum stress are indeed quite similar; therefore, the pressure distribution of contacts is not symmetrical with respect to the central plane, and the contact area on the right side becomes larger than that on the left side. Non-uniformity thus has a significant effect on pavement behavior, more precisely in bends where the relatively high vertical contact pressure of the tires could explain the accelerated pavement deterioration in curved road sections, which necessitate more frequent handling maneuvers.

Table 1: Contact area and average maximum stress vs. inclination

	Tekscan measurements		**SAM model**	
	Contact area (mm²)	Average maximum stress (kPa)	Contact area (mm²)	Average maximum stress (kPa)
0°	43,974	1,400	42,870	1,536
2°	53,471	1,591	52,370	1,650
4°	52,748	1,788	51,581	1,850
5°	51,845	1,859	50,081	2,000
6°	50,064	1,917	48,281	2,090

Moreover, the evolution in the average maximum vertical contact stress can be analyzed as a function of the variation in the angle of inclination. Figure 7 shows that the average maximum contact pressure increases as the angle of inclination increases; however, as 5° the pressures tend to stabilize. The calculated and measured maximum vertical stresses appear to peak at an inclination angle of 5°. Theoretically, it can be deduced that the maximum resistance of the tire is also reached at 5°. The design of the pavement's vertical resistance must be based on the maximum possible angle of inclination, which generates the most critical stresses (i.e. 5° in the present case).

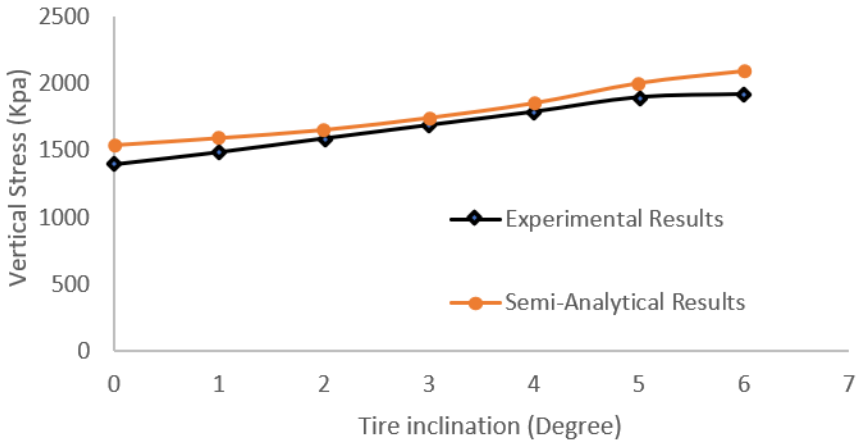

Fig. 7: Tire inclination angle: maximum vertical stress

3.3. Contact shear stress

This section will present the contact shear distribution in the case of break and rollover or a roundabout with a tire lean in the bend. During braking, a braking torque is applied in the opposite direction to the rolling direction (Fig. 8, left), with the angular velocity ωR becoming lower compared to the translation velocity ϑ (ωR < ϑ) and the relative rigid body slip turning negative.

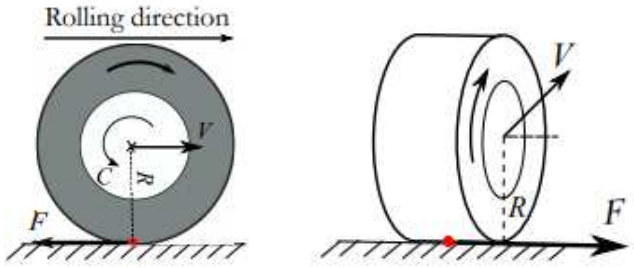

Fig. 8: (left) wheel braking by application of torque C, (right) free wheel during turning

A braking force is thus created. In the presence of friction, a surface shear causes the phenomenon of micro-slip on the contact surface. The shear stress field then tends to be in compression behind the contact zone. In turns or roundabouts, truck tires are subjected to lateral loads (Fig. 8, right) due to inertia and, in some cases, longitudinal traction loads during acceleration on slopes. An isolated free truck wheel in turning or at a roundabout is considered here. With normal force W = 45 kN, a longitudinal tangential load Q_x = -10 kN (Q_y = 5 kN) is applied for various angles. When the tire is subjected to a turning load of -10 kN and a transverse load of 5 kN at a tire inclination of 2°, a longitudinal shear stress representation shows (Fig. 9) that the slip zone lies at the front of the contact area. In contrast, the shear value is negative, which causes compression of the pavement surface while the maximum transverse stresses are located at the outer edge of the tire. For a tire inclination of 5°, the compressive (longitudinal) stresses in the sliding zone have greatly increased compared to the results at 2°. The transverse stresses have also slightly increased, with a concentration on the outer edge of the tire. The shear stresses for 6° do not change compared to 5° for the normal tire, which confirms the vertical stress evolution curve vs. angle of inclination, where stabilization as of 5° has been observed. Similarly, the shearing zone for

transverse stresses did not evolve compared to the calculations at 5°. Results of the semi-analytical calculations indicate that the maximum shear stress increases with an increase in the angle of tire inclination from 0° to 5°, which provides further evidence to support the theoretical hypothesis that traffic in a cornering configuration can cause higher shear stresses on the pavement surface. Since one of the causes of rutting is shear strain, pavement sections where traffic turns (e.g. intersections) may therefore be more prone to surface rutting breaks. Figure 9 also shows that at an inclination angle of 5°, the shear stress is maximized. Like for vertical pressures, the design of the HMA shear strength should also be based on the maximum possible tilt angle, responsible for generating the most critical stresses, i.e. again in this case 5°.

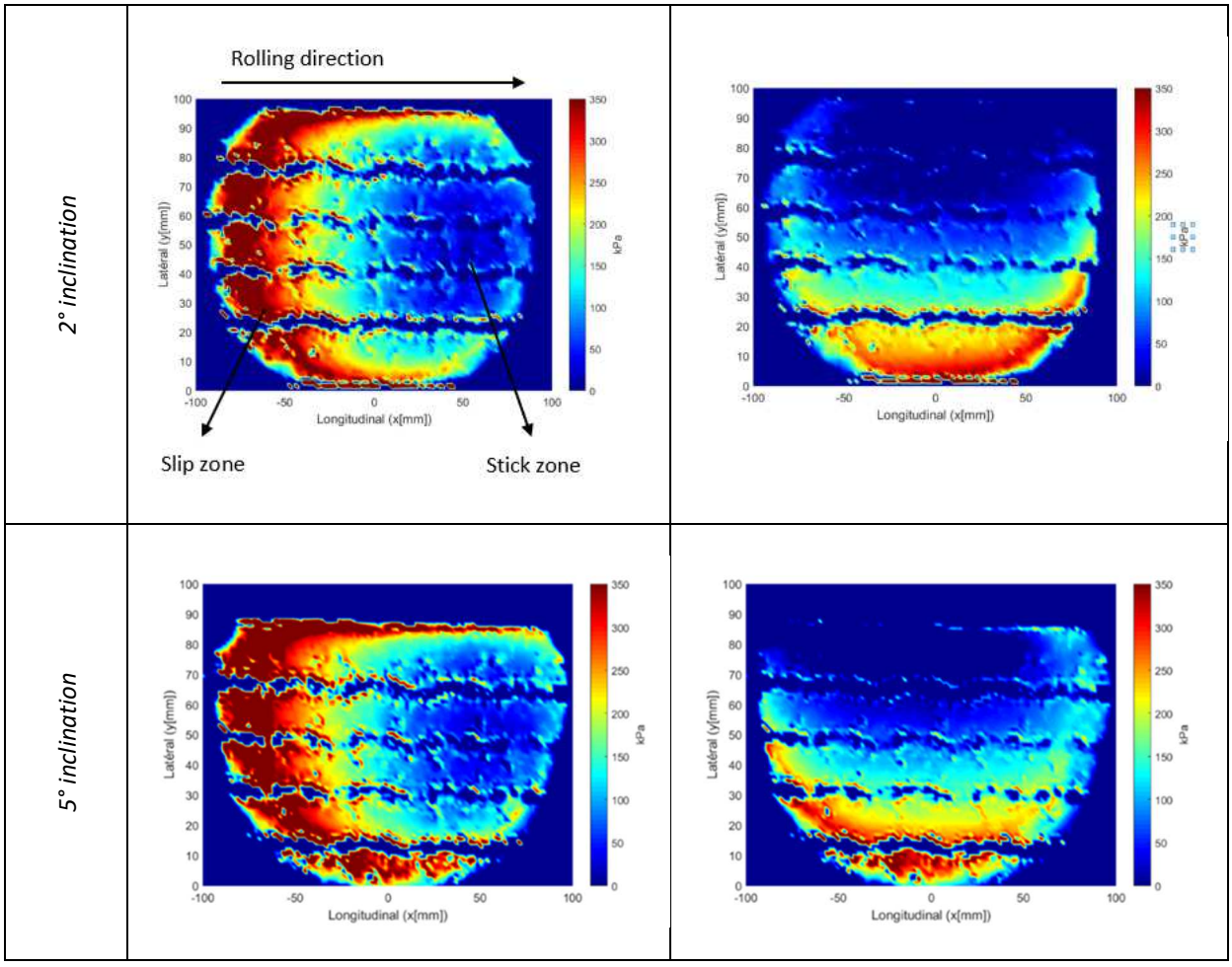

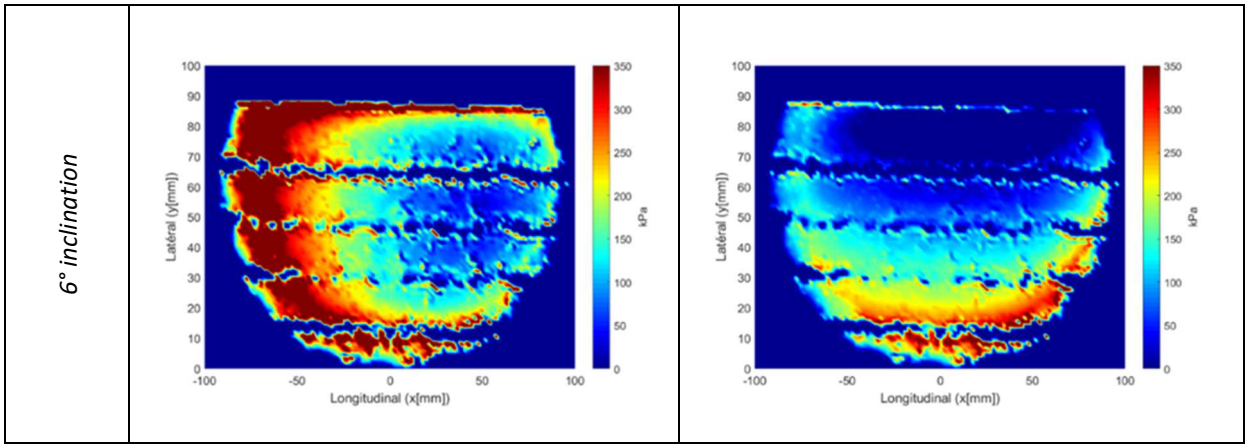

Fig 9: (right) transverse surface shear stress, (left) longitudinal surface shear stress (z=0)

3.4. Contact shear strain

To identify the critical factors exerting a significant impact on the mechanical behavior of pavement in a bend, the evolution of the principal tensile strain is also analyzed vs. the angle of tire inclination. The shear strain in the case of a break and rollover or roundabout with tire lean during cornering, with the variation in tire tilt angle, is included in this analysis. Results of the semi-analytical calculation of the principal strain in the traction rolling surface layer along a normal section (0°) and in bends with tire inclination (2°) are displayed in Figure 10. On a normal section, the most severe principal strain distribution has occurred near the edge of the tire load, with a maximum strain of 200 µstrain, as shown in Figure 10a.

However, the distribution of the shear effect zone has shifted to the inner edge of the tire by tilting the tire load with an increasing strain (Fig. 10b) for the 2° tire tilt. The displacement of the zone where the principal strain is reported could indicate that the critical shear failure zone extends over the entire width of the tire contact zone, as a function of the tire inclination, which may partially contribute to surface layer rutting. In the case of a 4° tire inclination (Fig. 10b), the principal strains are produced at the inside edge of the tire-road contact, with a maximum strain of 280 µstrain. At 5°, the maximum strains always concentrate on the inner edges of the tire but with an increase in the maximum strain, which rises from 320 µstrain at 4° to 360 µstrain at 5° (Fig. 10d). It has been effectively demonstrated that the fatigue cracks from above mainly appeared due to the stresses induced by the tire-pavement contact [2]. Major tangential forces can be exerted on the surface layer, resulting in significant tensile and shear stresses, which are responsible for the initiation of surface cracks [30].

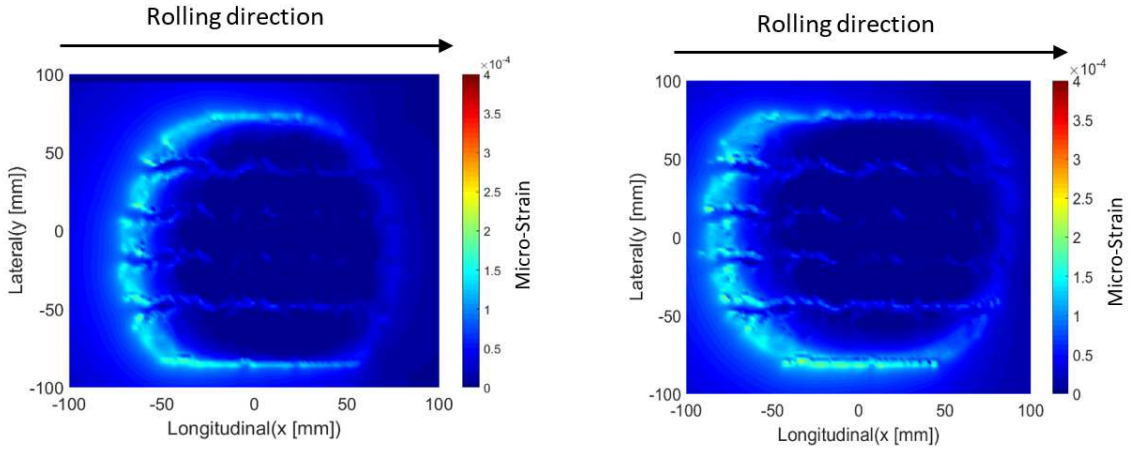

a) Principal strain at 0° b) Principal strain at 2°

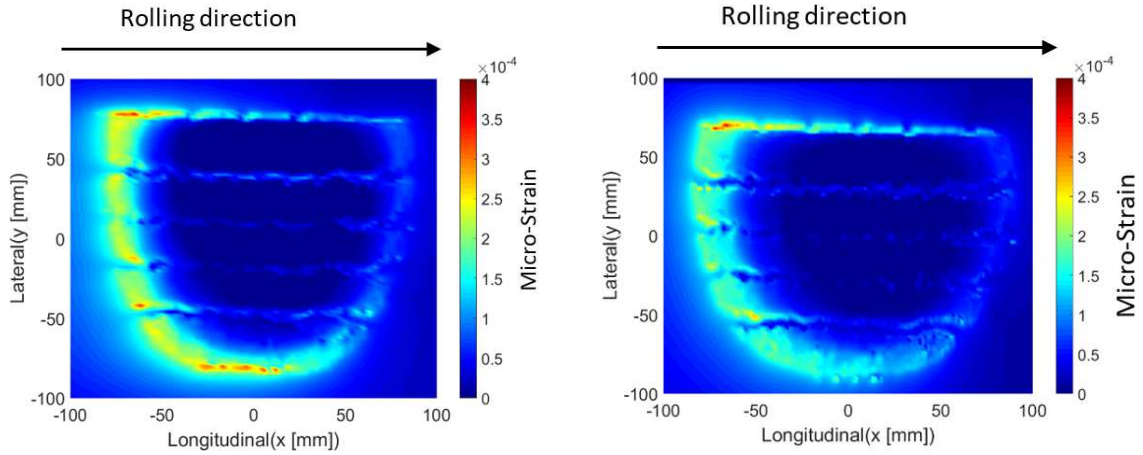

c) Principal strain at 4° d) Principal strain at 5°

Fig 10: Principal strains at 0°, 2°, 4° and 5° (z=0)

These conclusions have also been demonstrated by other authors. With a viscoelastic modeling assumption and non-uniform contact pressures, Bai et al. [31] proved that the surface layer is more susceptible to failure due to high shear stresses at the surface. Xiaodi et al. [32] used finite element modeling in the framework of an actual tire-pavement contact distribution. Results showed that the critical location of cracks due to maximum tensile stresses always appears to be close to the tire edge or in the tire-pavement contact area. Downward cracking is then caused by the traffic load occurring near or inside the wheel tracks in the direction of rolling.

The French pavement design method [33] assumes that strain cracking is of the tensile type. This method evaluates the tensile strain ε_t at the bottom of an asphalt concrete (AC) layer in order to predict the load cycle of bottom cracking by means of Equation (5).

$$\varepsilon_t = \leq \varepsilon_{6(10°C,25Hz)} \cdot \left(\left(\frac{E_{(10°C,10Hz)}}{E_{(15°C,10Hz)}}\right)^{0.5} \cdot \left(\frac{N_f}{10^6}\right)^{b} \cdot k_r \cdot k_c \cdot k_s \right) \quad (5)$$

where:

$\varepsilon_{6(10°C,25Hz)}$: Strain level at failure after one million cycles (10^6)

$E_{(10°C,10Hz)}$: Elastic modulus at 10°C, 10 Hz

$E_{(15°C,10Hz)}$: Elastic modulus at 15°C, 10 Hz

N_f: Number of equivalent standard axles for bottom cracking

b: Slope of the fatigue law (in $\log \varepsilon_t - \log N_f$)

k_r: Variability coefficient, i.e. a function of calculation risk and scattering factors

k_c: Fitting coefficient between numerical design and field observations

k_s: Coefficient for heterogeneity in soil bearing capacity.

These parameters are determined by laboratory fatigue tests. The major parameter in this model is ε_6, which characterizes the lifetime threshold of one million cycles, beyond which the crack is accelerated depending on the bituminous mixture. The strain level ε_6 (10°C, 25 Hz) at failure after one million cycles on the bituminous mixture (BBSG) used for purposes of this calculation is about 100 µstrain. According to the above results, the maximum micro-

strain moves towards the outer edge of the tire as the angle of inclination increases, with maximum strains exceeding ε_6. Once again, this value is more than twice ε_6 by fatigue, with respect to the asphalt life cycle, and more limited top-down cracking starts to appear. The traction is concentrated towards one side of the contact zone, in the direction of the load application. Figure 11 shows the primary traction directions at a tire inclination of 4°.

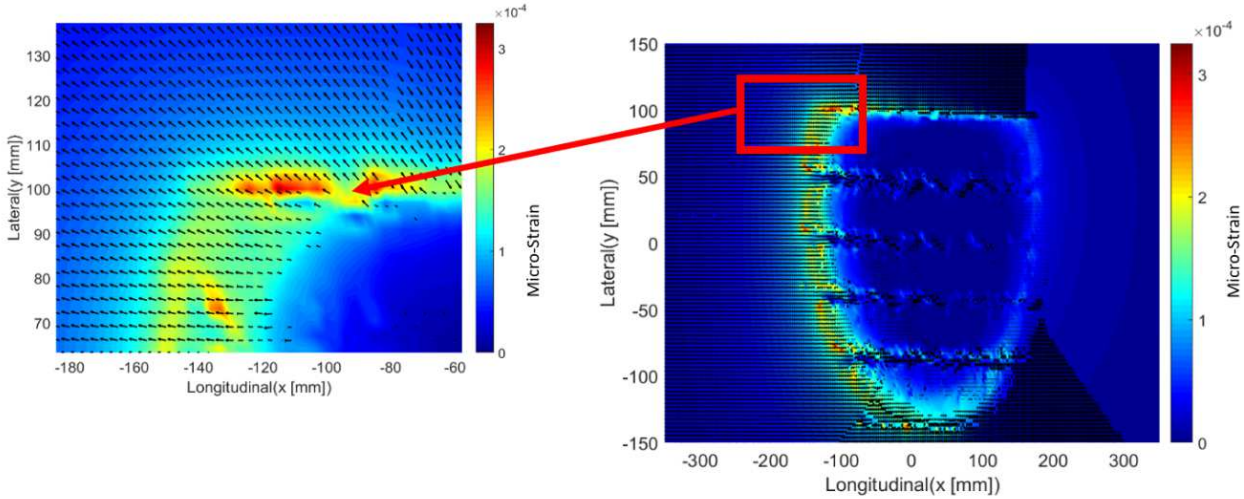

Fig 11: Principal surface strain directions (z = 0) in the turning section with a 4° inclination

Given this configuration, longitudinal top-down cracking will occur towards the outer side during turning or on a roundabout.

Conclusion

This paper has introduced the modeling and validation for application of a semi-analytical method used to analyze tire-pavement rolling contact in a road's bend sections. Such a code provides the advantage of a more realistic, accurate and faster calculation than current methods, which include the Finite Element Method (FEM). The model developed herein thus makes it possible to obtain the contact pressure while cornering when stresses are assumed to be maximized. Based on the simulation results and experimental validation, the key findings, conclusions and recommendations drawn from this paper are summarized as follows:

- The contact pressure increases with an increase in the tire angle of inclination from 0° to 5°, although as of 5° pressures tend to stabilize.

- During traction rolling, the tire contact area contains two distinct zones: the stick zone in the front of the contact area, and the slip zone behind the contact area where the pavement surface exhibits different behavior. The shear stresses for an actual tire and a smooth tire increase considerably at a higher bank angle in the turn, but as of 5° they tend to stabilize for the vertical stresses. This finding serves as analytical evidence to support the theoretical hypothesis that traffic turning on roads (e.g. at intersections) can cause greater shear stress in the pavement than by other traffic patterns.

- In the normal section, the principal strain is located at the edge of the tire; moreover, when cornering, strain gets concentrated at the inside edge with an increase in the angle of inclination. This finding suggests that highway sections with large traffic volumes in their turns may be more susceptible to top-down cracking and surfacing rutting.

In conclusion, our model will lead to a better understanding of the performance of a pavement at specific points like bends, allowing for an analysis of shear stresses and the principal strain on the surface. These results can be incorporated into the pavement design methods in order to extend the surface layer life cycle. The semi-analytical model introduced in this paper offers a key advantage in terms of computing time and moreover proves to be a more precise tool as regards the contact area when using the actual tire profile.
Future work is planned to refine these results by modeling a multilayer pavement structure and considering the viscoelastic behavior of bituminous layers (in particular the surface layer). Also, the validation on a traffic simulator, a step that is currently underway, will consolidate all of these results.

References

[1] M. de Beer, C. Fisher, F. Jooste, Determination of Pneumatic Tyre/Pavement Interface Contact Stresses under Moving Loads and Some Effects on Pavements with Thin Asphalt Surfacing Layers Proceedings of the 8th International Conference on Asphalt Pavements (ICAP '97), Seattle, WA, 1997.

[2] R. Blab et J. T. Harvey, Modeling Measured 3D Tire Contact Stresses in a Viscoelastic FE Pavement Model, Int. J. Geomech. 2 (2002), 271-290. doi:10.1061/(ASCE)1532-3641(2002)2:3(271).

[3] J. A. Prozzi et R. Luo, Quantification of the Joint Effect of Wheel Load and Tire Inflation Pressure on Pavement Response, Transp. Res. Rec. J. Transp. Res. Board. 1919 (2005) 134-141. doi: 10.1177/0361198105191900114.

[4] Q. Liu et A. Shalaby, Simulation of pavement response to tire pressure and shape of contact area, Can. J. Civ. Eng. 40 (2013) 236-242. doi: 10.1139/cjce-2011-0567.

[5] X. Hu, A.N.M. Faruk, J. Zhang, MI. Souliman, LF. Walubita, Effects of tire inclination (turning traffic) and dynamic loading on the pavement stress–strain responses using 3-D finite element modeling, International Journal of Pavement Research and Technology 10 (2017), 304-314. doi.org/10.1016/j.ijprt.2017.04.005

[6] S.I. Lee, A.D. Mwanza, G. Mutembo, et L.F. Walubita, Effects of Tire Inclination on the HMA Pavement Shear Stress-Strain Response: 2-D Computational Modeling, in Design, Analysis, and Asphalt Material Characterization for Road and Airfield Pavements, Yichang, Hubei, China. (2014) 41-48, doi: 10.1061/9780784478462.006.

[7] H. Wang, I.L. Al-Qadi, et I. Stanciulescu, Simulation of tyre–pavement interaction for predicting contact stresses at static and various rolling conditions, Int. J. Pavement Eng. 13 (2012) 310-321. doi: 10.1080/10298436.2011.565767.

[8] H. Wang, I.L. Al-Qadi, et I. Stanciulescu, Effect of Surface Friction on Tire–Pavement Contact Stresses during Vehicle Maneuvering, J. Eng. Mech., 140 (2014) 04014001. doi: 10.1061/(ASCE)EM.1943-7889.0000691.

[9] J.A. Hernandez, A. Gamez, M. Shakiba, and I.L. Al-Qadi, Numerical prediction of three-dimensional tire-pavement contact stresses, Report ICT-17-004 (2004).

[10] P. Gruber, R.S. Sharp, and A.D. Crocombe, Friction and camber influences on the static stiffness properties of a racing tyre, Proc. Inst. Mech. Eng. Part J. Automob. Eng. 222 (2008) 1965-1976. doi: 10.1243/09544070JAUTO872.

[11] G. Yanjin, Z. Guoqun, et C. Gang, FEA and Testing Studies on Static Camber Performance of the Radial Tire, J. Reinf. Plast. Compos. 26 (2007) 1921-1936.

[12] H. Zhou, G. Wang, Y. Ding, J. Yang, C. Liang, et J. Fu, Effect of Friction Model and Tire Maneuvering on Tire-Pavement Contact Stress, Adv. Mater. Sci. Eng. 2015 (2015) 1-11. doi: 10.1155/2015/632647.

[13] G. Cheng, W. Wang, G. Zhao, Y. Guan, Z. Wang, Influence of Camber Angle on Rolling Radial Tire under Braking State, Procedia Engineering 15 (2011) 4310-4315. doi:10.1016/j.proeng.2011.08.809

[14] M. Vayalat, Tire Contact Patch Characterization through Finite Element Modeling and Experimental Testing, PhD dissertation, faculty of the Virginia Polytechnic Institute and State (2016).

[15] I. Kageyama, A study on tire modeling for camber thrust and camber torque, JSAE Rev. 23 (2002), 325-331. doi: 10.1016/S0389-4304(02)00204-7.

[16] Z. Ambassa, F. Allou, C. Petit, R. Medjo Eko, Evaluation de l'agressivité du trafic sur des chaussées bitumineuses en carrefour giratoire, Bull. Lab. Ponts Chaussées 280-281 (2013) 171-188.

[17] C. Petit, M. Diakhaté, A. Millien, A. Phelipot-Mardelé, et B. Pouteau, Pavement Design for Curved Road Sections: Fatigue Performance of Interfaces and Longitudinal Top-down Cracking in Multilayered Pavements, Road Mater. Pavement Des. 10 (2009) 609-624. doi: 10.1080/14680629.2009.9690216.

[18] M. Ziefle et U. Nackenhorst, Numerical techniques for rolling rubber wheels: treatment of inelastic material properties and frictional contact, Comput. Mech. 42 (2008) 337-356. doi: 10.1007/s00466-008-0243-9.

[19] S. Liu, Q. Wang, G. Liu, A versatile method of discrete convolution and FF (DC-FFT) for contact analyses, Wear 243 (2000) 101-111.

[20] I. Polonsky, L. Keer, A numerical method for solving rough contact problems based on the multi-level multi-summation and conjugate gradient techniques, Wear 231 (1999) 206 – 219.

[21] C. Jacq, D. Nélias, G. Lormand, D. Girodin, Development of a three-dimensional semi-analytical elastic-plastic contact code, ASME Journal of Tribology 124 (2002) 653–667.

[22] D. Nélias, E. Antaluca, V. Boucly, Rolling of an elastic ellipsoid upon an elasticplastic flat, ASME Journal of Tribology, 129 (2007) 791–800.

[23] D. Nélias, E. Antaluca, V. Boucly, S. Cretu, A 3D semi-analytical model for elastic plastic sliding contacts, ASME Journal of Tribology 129 (2007) 761–771.

[24] L. Gallego, D. Nelias, S. Deyber, A fast and efficient contact algorithm for fretting problems applied to fretting modes I, II and III, Wear, 268 (2000) 208-222.

[25] J. Boussinesq, Application des Potentiels à l'Etude de l'Equilibre et du Mouvement des Solides Elastiques, In French, Gauthier-Villars, Paris (1885).

[26] EY. Manyo, P. Reynaud, B. Picoux, R. Tautou, D. Nelias, F. Allou, C. Petit, Towards fast modelling of the tire-pavement contact, European Journal of Environmental and Civil Engineering, (2019) . doi: 10.1080/19648189.2019.1628812.

[27] V. Cerruti, Ricerche intorno all'equilibrio de' corpi elastici isotropi", Rend. Accad. Lincei. 3 (1882) 81–122.

[28] A.E.H. Love, A Treatise on the Mathematical Theory of Elasticity, 4th edition, Cambridge University Press, London (1952).

[29] G. Duvaut, J.L. Lions, Les Inéquations en Mécanique et en Physique, In French, Dunod, Paris (1972).

489 [30] E. Freitas, P. Pereira, L. Picado-Santos, Assessment of Top-Down Cracking Causes in
490 Asphalt Pavements. Maintenance and Rehabilitation of Pavements and Technological
491 Control, University of Minho, Guimaraes, Portugal (2003).
492 [31] T. Bai, Z. Cheng, X. Hu, L. Fuentes, L. F. Walubita, Viscoelastic modelling of an asphalt
493 pavement based on actual tire-pavement contact pressure, Road Mater. Pavement Des. (2020),
494 doi: 10.1080/14680629.2020.1766545.
495 [32] X. Hu and L. F. Walubita, Modelling Tensile Strain Response in Asphalt Pavements:
496 Bottom-up and/or Top-down Fatigue Crack Initiation, Road Mater. Pavement Des. 10 (2009)
497 125-154, doi: 10.1080/14680629.2009.9690185.
498 [33] SETRA-LCPC, Conception et dimensionnement des structures de chaussée, guide tech
499 Edition, Paris, France (1994).